

Development and characterization of the Capillary DirectINJECT System

Jurek Parodi¹

Bionetics, NASA Ames Research Center, Moffett Field, CA, 94035

Sofia Fanourakis², John Vance³

KBR, NASA Ames Research Center, Moffett Field, CA, 94035

and

Lance Delzeit⁴

NASA Ames Research Center, Moffett Field, CA, 94035

The DirectINJECT Project was initiated to develop a reliable in-line dosing system to deliver a concentrated silver ion biocide solution at ultra-low flow rates into spacecraft potable water. Three dosing systems, employing a miniature peristaltic pump, a multi-piston pump, and differential pressure-driven flow through a capillary tube, were quickly prototyped and tested. Although the peristaltic and multi-piston pump systems met the desired flow rate range, the capillary system showed the most promise and was chosen for further development. In FY23, the Capillary DirectINJECT dosing system underwent extensive testing with a nominal injection rate of 1.0 $\mu\text{l}/\text{min}$ into varying backpressure conditions. A Primary DirectINJECT System with triplicate testbeds was employed for long-term testing, and auxiliary systems including the Secondary DirectINJECT System and Leak Testbed were developed to characterize specific components and investigate various phenomena related to the dosing system. Parameters such as flow rates, reservoir pressures, and temperature were monitored throughout the testing campaigns.

Nomenclature

$^{\circ}\text{C}$	=	degree Celsius
Ag^+	=	silver ion
AgNO_3	=	silver nitrate
<i>COTS</i>	=	commercial off-the-shelf
<i>DI</i>	=	deionized
ΔP	=	pressure differential
ΔT	=	temperature differential
<i>ETFE</i>	=	Ethylene tetrafluoroethylene
<i>FFKM</i>	=	perfluoroelastomer
<i>FY</i>	=	fiscal year
<i>g</i>	=	grams
<i>gal</i>	=	gallon
<i>GPD</i>	=	gallons per day
<i>H₂O</i>	=	water
<i>Hz</i>	=	Hertz
<i>ID</i>	=	internal diameter

¹ Project Engineer, Bioengineering Branch, NASA ARC N239-15, Moffett Field, CA 94035.

² Research Scientist, Bioengineering Branch, NASA ARC N239-15, Moffett Field, CA 94035.

³ Research Engineer, Bioengineering Branch, NASA ARC N239-15, Moffett Field, CA 94035.

⁴ Physical Scientist, Bioengineering Branch, NASA ARC N239-15, Moffett Field, CA 94035.

<i>ISS</i>	= International Space Station
<i>Kg</i>	= kilograms
<i>l</i>	= liter
<i>mA</i>	= milliampere
<i>min</i>	= minute
<i>ml</i>	= milliliter
<i>ms</i>	= millisecond
<i>μl</i>	= microliters
<i>μm</i>	= micrometers
<i>N₂</i>	= nitrogen gas
<i>ppb</i>	= parts per billion
<i>PEEK</i>	= polyether ether ketone
<i>P/N</i>	= part number
<i>P&ID</i>	= piping and instrumentation diagram
<i>psi</i>	= pounds per square inch
<i>psia</i>	= pounds per square inch absolute
<i>psig</i>	= pounds per square inch gauge
<i>RTD</i>	= resistance temperature detector
<i>WPA</i>	= Water Processing Assembly

I. Introduction

THE DirectINJECT Project was started in fiscal year 2021 (FY21) to develop a reliable in-line dosing system to enable the continuous, ultra-low flow rate delivery of a concentrated silver ion (Ag⁺) biocide solution into the potable water stream produced by spacecraft water processing hardware. In FY22, three alternative dosing systems were rapidly prototyped and tested, employing: 1) a differential pressure-driven flow through a micro-capillary tube, 2) a miniature peristaltic pump, and 3) a multi-piston pump with four integrated miniature pistons.¹

Based on the nominal 100 ml/min potable water production rate used in the International Space Station (ISS) Water Processing Assembly (WPA) and on the desired biocide concentration of 400 ppb Ag⁺ in the effluent, a 40 g/l Ag⁺ concentrate was selected with a targeted dose rate of 1.0 μl/min (dilution ratio of 1:100,000). Assuming a 2,000-liter water consumption per crew-year (5.5 l/crew-day), the consumption of biocide solution in this operational scenario would be only 20 ml/crew-year.

Preliminary experiments confirmed that all three systems could dose deionized water at the desired ~1.0 μl/min flow rate into ambient pressure, and that all systems could pump into 3 psi backpressure. Both the peristaltic and multi-piston pump systems were able to dose with average rates in the range of 0.1-5 and 0.2-10 μl/min, respectively, by varying the rotational speed, while the capillary system flow rate was controlled by either varying the pressure of the supply reservoir or by pulse-width modulation of the solenoid shut-off valve. A 7-day experiment with 40 g/l Ag⁺ (from AgNO₃) was completed to investigate short-term reliability and materials compatibility, confirming that Ag⁺ loss during continuous flow-through is minimal. However, the dosing profiles were very different between the three systems, with both pump systems having a pumping profile with periodical variations over periods of several seconds to a few minutes. The capillary system, instead, had constant flow of silver ion biocide solution with no periodical variations in delivery.

In FY23, the most promising dosing system among the three alternatives was selected *a priori* for further development and testing. This preliminary selection process was due to an announced programmatic trade study scheduled for FY24 and was guided by the following factors:

- 1) The micro-peristaltic pump offers a nominal operational lifetime of only 1000-2000 hours (equivalent to 2-8 months) before stepper motor failure. Moreover, the potential failures of the peristaltic tubing could lead to the unintended release of concentrated silver biocide solution with limited means of detecting such events. Given that a journey to Mars typically takes around 12 months, multiple tubing replacements might be necessary. Finally, the pumping profile of this system might require a more complex mixing/stirring setup. Due to the tubing issue and the uncertain lifespan of the motor, the micro-peristaltic pump was excluded from consideration.
- 2) The multi-piston pump displayed an acceptable pumping profile, yet it is a complex electromechanical system. Although the system specifications seemed suitable, concerns arose regarding potential unforeseen problems caused by leakage across the piston seal and associated mechanical wear. Given

the demanding development timeline, these wear-related concerns, while deemed of moderate risk, were significant enough to rank this system as the second choice and to hold it as a backup to the capillary system.

- 3) The capillary system's lack of moving parts (except for the solenoid valve and the piston in the supply tank), and its ability to provide constant flow of silver ion biocide solution with no periodical variations in delivery, led to its selection as the optimal choice for the DirectINJECT doser.

Work accomplished in FY23 includes long-duration testing campaigns on the Capillary DirectINJECT dosing system to investigate the performance and reliability of its main components using a nominal injection rate of 1.0 $\mu\text{l}/\text{min}$ of deionized (DI) water into a broad range of backpressure (3 psig and 30 psig). Flow rates, inlet and outlet reservoir pressures, and temperature of ambient air and specific components, were recorded at a minimum frequency of 0.2 Hz. A Primary DirectINJECT System composed of two triplicate testbeds was built and used for long-term testing. Other auxiliary systems (Secondary DirectINJECT System, Leak Testbed) were developed and used to characterize specific components such as solenoid valves and capillary tubes, and to investigate phenomena of interest, such as leak rates of different reservoir/piston designs, two-phase flow of gas super-saturated solutions, and larger capillary diameters.

Finally, the preliminary design of an ISS-like DirectINJECT prototype system operating under the range of conditions expected for the WPA on the ISS was completed.

II. Development and Characterization of the Capillary DirectINJECT System

A. Background

The Capillary DirectINJECT System is based on pressure-driven flow of a concentrated Ag^+ biocide solution through a micro-capillary tube supplied by a pressurized reservoir. The laminar flow of an incompressible fluid through a cylindrical capillary tube is governed by the Hagen-Poiseuille law, shown in Eq. (1):

$$Q = \Delta P \pi R^4 / 8 \eta L \quad (1)$$

where Q is the volumetric flow rate, ΔP is the pressure differential across the tube, R is the internal tube radius, η is the dynamic viscosity, and L is tube length. With the tube dimensions being constant, the flow rate can be set by a pressure difference between tube inlet and tube outlet, and by adjusting it to take into account the viscosity of the solution, which is function of its temperature.

Assuming a nominal spacecraft cabin temperature of 22.5°C and the required temperature range of 18-27 °C (according to NASA STD 3001 Vol 2 Rev B and to the NASA Human Integration Design Handbook), the consequent theoretical flow rate variation due to changes in viscosity was expected to be in the order of approximately +/-10%, which would neither affect the biocidal effectiveness on the stored potable water at the lower concentration of 360 ppb, nor the health of the astronauts at the potential higher intake of 440 ppb. Generally, the cabin temperature on board the ISS ranges within +/- 2.0°C of the nominal value,² meaning that the consequent theoretical flow rate variation would be approximately +/-5%.

Thus, an actively controlled system that implements electronically controlled pressure regulators or solenoid valves with variable duty cycles would not be necessary (assuming a relatively constant potable water production rate), maximizing system simplicity.

B. Materials and System Design

The capillary dosing systems developed for this project were constructed entirely from commercial off-the-shelf (COTS) parts. In a flight system, the pressurizing gas would most likely be supplied by the ISS compressed nitrogen (N_2) bus. However, in order to reduce costs and simplify operations, a 1 stage horizontal air compressor with a 12-gal tank (GAST part # 3HBB-69T-M300AX) was used to supply the required compressed gas to both the Primary and the Secondary DirectINJECT Systems, and to the Leak Testbed. Much of the other hardware used during this year's testing campaigns would most likely be used in a final flight system. The piping and instrumentation diagram (P&ID) of the original configuration of the Primary and the Auxiliary DirectINJECT Systems is shown in Figure 1. The system was certified for pressure safety prior to starting operations.

Both the Primary and Auxiliary systems of the Capillary Testbed implement pressurized reservoirs on both the inlet side and outlet side of the capillary tube, which were denominated as supply tanks and collecting tanks, respectively. The collecting tanks were pressurized at the lower pressure of 2.5 psig and 30 psig to simulate the

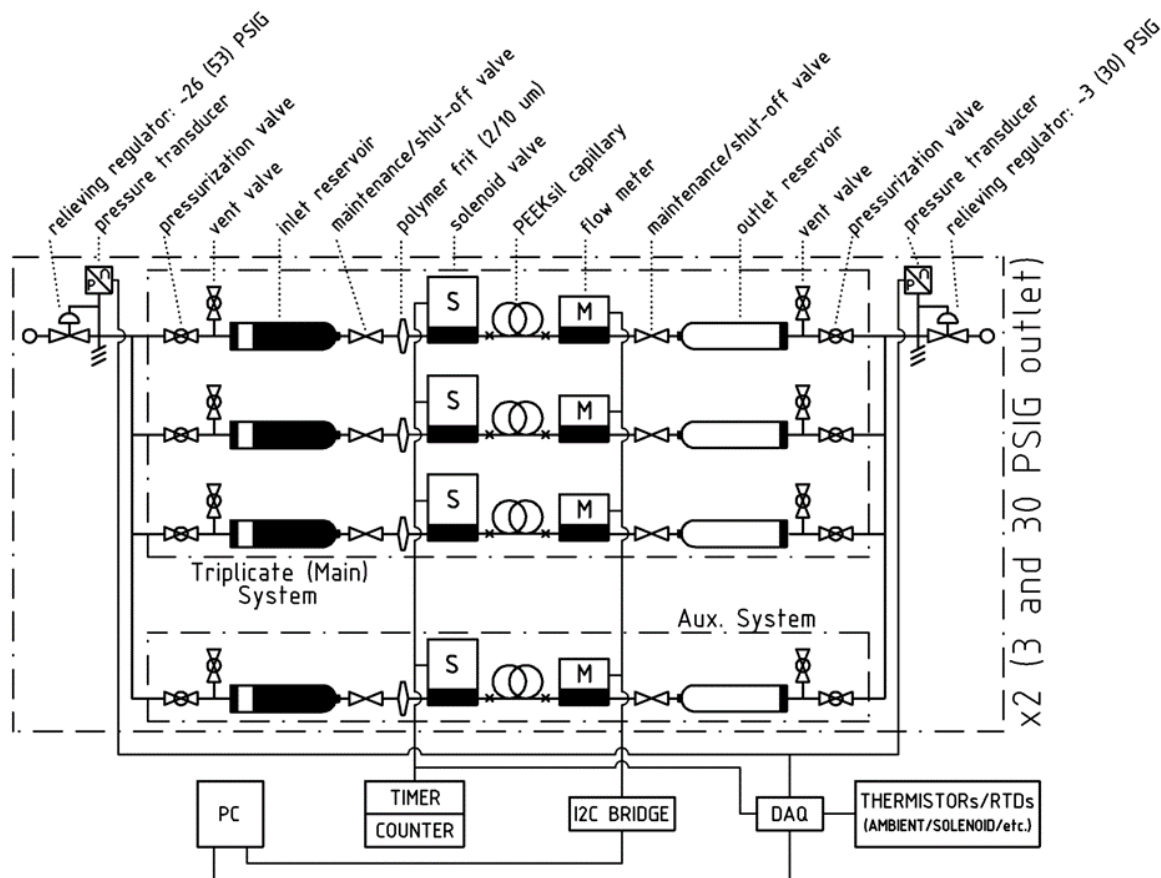


Figure 1. P&ID of the initial configuration of the Primary and the Auxiliary DirectINJECT Systems.

operational backpressure extremes of the WPA, while the supply tanks were pressurized at the higher pressure necessary to achieve the desired theoretical flow of $1.0 \mu\text{l}/\text{min}$ (*respectively 27.5 psig and 55 psig*).

Two sets of 4 manual-loading pressure regulators with ranges of 0-35 psig (ITT Conoflow, part # GH10XTHEAXAD) and 0-60 psig (ITT Conoflow, part # GH10XTHEAXAF), each with their ancillary hardware comprised of shut-off valves, pressure relieve valves, mufflers, and plumbing are used to independently set and adjust the supply and collecting tanks pressures of the Primary and Auxiliary DirectINJECT Systems at the desired values, allowing to simultaneously run separate experiments on both systems. The 8 manual loading pressure regulators have a sensitivity of $7 * 10^{-3}$ psi and a supply pressure effect of 0.1 psi for 25 psi change in supply pressure (Figure 2). They are constant-bleed type regulators: at equilibrium, the force exerted by the range spring is balanced by the force from the output pressure acting underneath the diaphragm assembly, but if the output pressure rises above the set pressure, the diaphragm seat is lifted from the nozzle plug, venting the excess pressure to atmosphere until equilibrium is reached. If the output pressure drops below the set pressure, the unbalanced force from the range spring acts through the diaphragm assembly unseating the nozzle plug. This allows supply pressure to flow through the nozzle to the downstream port increasing the output pressure. The output pressure increases until it balances the force

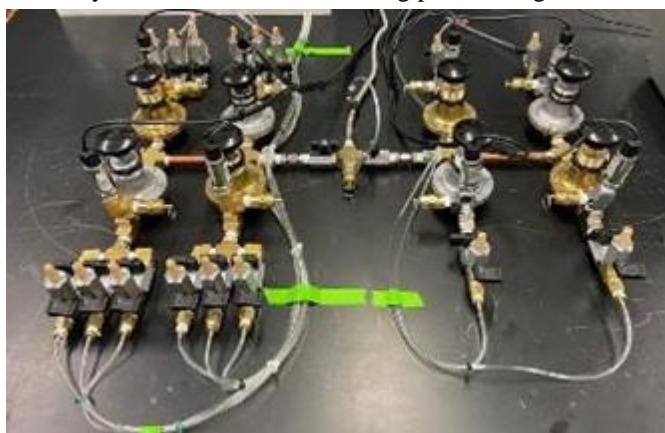


Figure 2. Primary and Auxiliary pressure regulators setup.

on the diaphragm assembly by the range spring. This type of regulator is usually used in applications where the flow demand is low. The constant bleed keeps the diaphragm in a dynamic state by preventing the nozzle from closing completely. This increases both the sensitivity and the stability of the regulator. At the current development level, this is a cheaper and acceptable choice for the Primary and Auxiliary DirectINJECT Systems. However, a flight system that will be pressurized using the ISS N₂ bus will require a no bleed/no relief diaphragm assembly that prevents the N₂ from exhausting to the cabin atmosphere. The principle of operation of a no bleed pressure regulator is the same except that the excess output excess pressure is relieved downstream instead of being vented to atmosphere as the diaphragm seat lifts off the plug and the nozzle closes.

The pressures are monitored and recorded using 0-30 psig and 0-100 psig pressure transducers (respectively Dwyer, part # 626-08-GH-P1-E1-S1 and Dwyer, part # 626-10-GH-P1-E1-S1) installed downstream of each pressure regulator and connected to a high-speed data acquisition (DAQ) USB board (Measurement Computing, part # USB-231) run from the DAQami application installed on a dedicated Windows laptop. The pressure transmitters convert a single positive pressure into a standard 4-20 mA output signal and have a full-scale accuracy of 0.25% (0.075 psi and 0.25 psi respectively for the low pressure and high-pressure transmitters) and a response time of 300 ms. The USB-231 DAQ board provides a dedicated input channel to each pressure transmitter and has a maximum continuous sample rate of 6,250 Hz per channel. As only the relative changes are important, all components are used as received.

A separate 8-channel temperature measurement device (Measurement Computing, part # USB-TEMP) is used to record temperatures from a thermistor and a resistance temperature detector (RTD). Each channel has a maximum sample rate of 2 Hz. Due to the intrinsic long-term nature operational scenario of the DirectINJECT Systems, this apparently limiting low frequency actually exceeds the data acquisition needs since the minimum duration for a meaningful experiment does not go below a few hours, with most experiments being run for days or weeks at the time. The USB-TEMP device was calibrated using the Insta-Cal utility to minimize the thermal drift between the two sensor categories, achieving an average temperature differential of 0.39°C between the thermistor and the RTD at ambient temperature. During the testing campaigns, the thermistors were used mainly to measure surface temperatures while the RTD, due to its higher stability, was used to record ambient temperature.

The 8 supply (6 on the Primary System and 2 on the Auxiliary System) and their respective 8 collecting tanks used as pressurized reservoirs are 50 ml polypropylene pneumatic dispensing syringes (Nordson EFD, part # 7012134) rated at 100 psig, with adapter assemblies (Nordson EFD, part # 7012056) plumbed with a flexible hose to their respective pressure regulators assemblies (Figure 3). Several pistons with different designs and tolerances are available depending on the application. The white, general purpose SmoothFlow, piston (Nordson EFD part # 7012186) made of high-density polyethylene was initially used during the testing and characterization of the Primary and Auxiliary systems. The outlet of the syringes connected via an 0.020" ID ETFE tubing (IDEX, part # 1516L) to a 10 µm pore PEEK frit filter contained in a PEEK holder (IDEX, part #s A-720 and A-355) to protect the capillary tube, followed by a normally closed miniature solenoid valve with connecting flange (Bürkert, part #s 273206 and 694895). The solenoid valve was selected due to its construction with inert and chemically resistant materials (PEEK body and FFKM diaphragm), low internal volume, and long cycle life rating claimed by the manufacturer (3×10^7 cycles under laboratory conditions). A 100 mm long, PEEK jacketed, fused silica micro-capillary tube with an inner diameter of 25 µm (PEEKsil™, IDEX part # 62510) is directly connected to the solenoid valve. The fused silica core provides a



Figure 3. Primary (left) and Auxiliary (right) DirectINJECT Systems.

consistent and rigid fluid pathway with very tight tolerances while the PEEK outer sheath is ideal for sealing with many styles of fittings. The pressure rating is determined by the inner diameter of the tubing and is 25,000 psig for this tubing and the ID tolerance claimed by the manufacturer is 1 μm . The outlet of the capillary tube was then connected to a flowmeter (Sensirion, part # LG16-0150D) with maximum flow rate of 7 $\mu\text{l}/\text{min}$ for water (H_2O) at 23°C and 14.5 psia. The accuracy below full scale is 5% of the measured value.

Since this a calorimetric flow meter, which is a type of thermal mass flow meter that measures the asymmetrical temperature of a fluid flow between two temperature sensors placed around a heating element, its reliability is very high due to the absence of moving parts. Its accuracy is affected by variations in temperature, heat capacity, and viscosity of the fluid.³ Thus, it is subject to an additional error of 0.09% of the measured value / °C (according to the manufacturer). This detail is relevant to explain some of the results obtained during the bubbles effect testing described later. The flow meter is factory calibrated for H_2O at 23°C. The temperature sensors are mounted symmetrically upstream and downstream of the heating element in the direction of flow. Any flow through the tube causes the thermal transfer of heat to the downstream temperature sensor, thus generating a precisely measurable signal due to the resulting difference in temperature. The higher the flow rate, the higher is the difference in temperature between the two sensors. The wetted path is composed of a straight-through capillary made of fused silica, with an ID of 150 μm , and a pressure rating of over 2,000 psig and a burst pressure over 4,000 psig. The rest of the body material is PEEK. The operating temperature range is 10°C to 50°C, with maximum short-term temperature peaks of 60°C. Digital communication between the flow meter and the data acquisition laptop runs via a standard I²C-interface and is controlled using Windows PowerShell. Response time to flow changes is 40 ms and the sampling time at 16-bit resolution is 76 ms. The flow readout frequency was adjusted for each experiment to match that of the DAQami.

Finally, the outlet of the flow meter is connected to the receiving tank via 0.020" ID ETFE tubing.

C. System Characterization

A first preliminary 12-hour test was conducted with all the Primary and Auxiliary supply tanks connected to a single pressure regulator, set at 25 psig. All the Primary and Auxiliary collecting tanks were open to ambient atmosphere (0 psig) but covered with parafilm. The flow rates were recorded from both systems using 2 separate USB inputs on the same laptop after several attempts to debug the PowerShell program. The data from the pressure transducers DAQ and the temperature DAQ was recorded on DAQami using the 2 remaining laptop USB inputs, using sample rates of 2 Hz. The average theoretical flow expected for these experimental conditions was 0.94 $\mu\text{l}/\text{min}$. 3 out of the 6 Primary testbeds did not have any flow at all during this run. The trendlines of the flows are shifted, resulting in different average flow rates over the 12 hours, as seen in Figure 4. However, the drop in flow over time corresponds to temperature drop overnight, as expected, and as shown in detail in Figure 5. The root cause of the different flows was believed to be either a constricted capillary tube due to either manufacturing tolerances or the over-torquing of its fittings, or to an obstructed/broken glass capillary in the flow meter. The root cause of the complete absence of flow was first believed to be due to failed solenoid valves. Thus, the next steps were to characterize the single system components since they were never tested

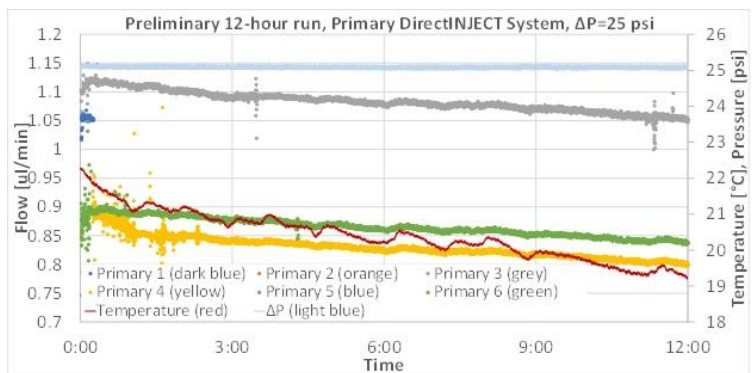


Figure 4. Flow rates and ambient temperature of preliminary 12-hour test. Pressure set at 25 psig, and all collecting tanks open to the atmosphere. Time is in hh:mm.

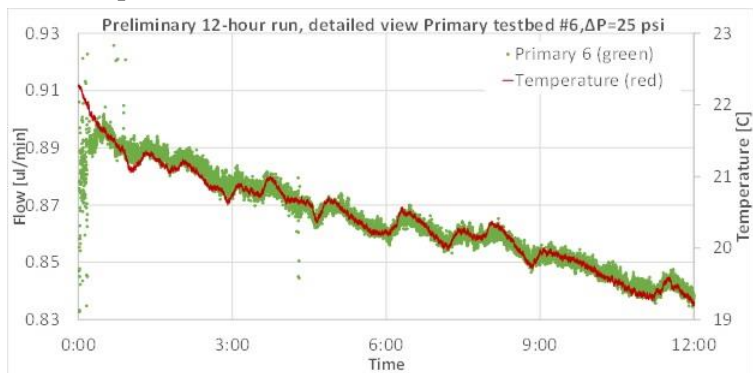


Figure 5. Detailed view from graph in Figure 4. Flow rate of Primary testbed #6 in function of temperature. Time is in hh:mm.

alone prior to their integration in the Primary and Auxiliary systems.

The Auxiliary system recorded random, off-range “3.072” $\mu\text{l}/\text{min}$ values throughout the run. The root cause of this glitch was believed to be either the sampling frequency set in the PowerShell program or a more likely bad electrical connection. The wiring was inspected and re-soldered, and the Auxiliary System was successively tested using different sampling frequencies.

The first components to be isolated and characterized were the solenoid valves. Due to the software glitch on the Auxiliary system that still had to be resolved, the test was conducted only on the 6 testbeds of the Primary system. All the Primary supply tanks were connected to a single pressure regulator, set at 7.5 psig, while all the Primary collecting tanks were open to ambient atmosphere but covered with parafilm (0 psig). The capillary tubes and the flow meters were bypassed. The solenoid valves initially closed. The supply tanks were completely drained before being filled with 10 ml of DI H_2O each.

The solenoid valves were then opened simultaneously, and the time was recorded for each collecting tank when filled completely. The time generally increased from run to run (with a few exceptions), indicating that the temperature of the solenoid valves, which heat up when opened, and which might not cool down to the original ambient temperature between runs, might affect the flow through the system. The heating of the solenoid valves likely causes an expansion of its internal materials that reduces the ID of the wet path, thus resulting in a lower flow. The maximum ΔT between the hottest and coldest solenoid valves during all the consecutive runs was about 5°C , or approximately 12% (Figure 6). Ambient temperature and applied pressure are excluded from the possible variables affecting this behavior since their variations are negligible during the duration of each test (about 4 minutes) and from one test to the other.

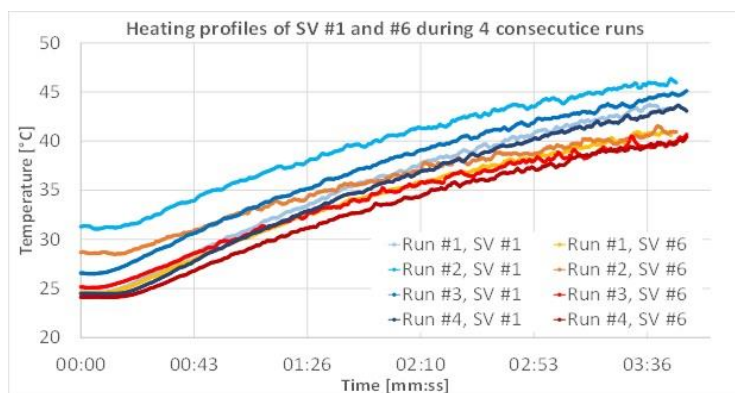


Figure 6. Comparison of the heating profiles of solenoid valve #1 (coldest) and #6 (hottest) during 4 consecutive runs.

The test was then repeated at a much lower pressure to measure the long-term temperature effects. The testbeds were completely drained before filling the supply tanks with 50 ml of DI water. The pressure regulator pressurizing the supply tanks was set at ~ 0.3 psig, while the collecting tanks were open to ambient atmosphere (0 psig). During the 18 hours of the test, no pressure drop was observed, and the temperature profiles of the solenoid valves reflected the drop of ambient temperature in the lab overnight, but their ΔT remained consistent. The overall trend remained similar to the previous short-term test, with the average ΔT between the hottest and coldest solenoid valves being 6.4°C , resulting in the hottest solenoid valve having the lowest flow and *vice versa*.

The solenoid valves characterization testing demonstrated that all the solenoid valves were working properly and thus they were not responsible for the complete absence of flow during the preliminary run, as previously hypothesized. Thus, the next components to be isolated and characterized were the capillary tubes and the flow meters. A single testbed on the Primary system was used to test all the capillary tubes and flow meters at $\Delta P = 20$ psi. The supply tank was filled with 10 ml of DI water and its pressure was set at 20 psig, while the collecting tank was open to ambient atmosphere, (0 psig). Every capillary tube was tested for 1 hour using the same flow meter, and then every flow meter was tested for 1 hour using the same capillary tube.

Two of the 3 capillary tubes that did not have any flow at all during the preliminary run worked nominally after they were re-plumbed to the testbed used in this testing campaign. Only 1 of them continued to not provide any flow. This capillary was replaced with a brand new one and the flow through the testbed was restored, indicating that it was most likely damaged during the system integration process. The results of this testing campaign indicate that the flow is capillary-tube-dependent since the flows for each tube overlap regardless of the flow meter used (see graph in Figure 7). Thus, the capillary tubes are the components ultimately responsible for the proper function and for the different flow rates observed in the different testbeds, since the laminar flow of an incompressible fluid through a cylindrical pipe is directly proportional to the fourth power of the radius of the pipe itself (R^4), as described by the Hagen-Poiseuille equation in Eq. (1). This excludes de-facto the flow meters and all the other components of the DirectINJECT system, although the solenoid valves might have a minor effect on the flow rate due to the heat transfer to the flowing solution. The variance between the different capillary tubes is due to manufacturing: the manufacturer lists an ID

tolerance of $\pm 1 \mu\text{m}$ ($\pm 4\%$). Based on the results of this characterization, the tubes used in the system have a calculated ID between approximately $23.75 \mu\text{m}$ and $26 \mu\text{m}$, thus a tolerance of -5% to $+4\%$ with respect to the nominal value.

An observation made during this testing is that it takes about 15 minutes for completing the priming and reaching a steady state with constant, stable flow after draining the system between each run.

While repeating the testing campaign above at the lower ΔP of 3 psi, it was observed that while the flow meter was recording a positive flow rate close to the expected theoretical value, during certain runs, the receiving tank was not filling up with any DI water. The volume of DI water in the supply tank was decreasing and there were no apparent leaks in the system, thus violating the law of conservation of mass. During the subsequent investigation, it was noticed that by increasing the ΔP to 25 psi, the leaking became evident around a fitting and a shut-off valve, which was caused by stripped threads and low tolerance between the stem and the body of the valve

(Figure 8). It was determined that at $\Delta P = 3$ psi, the system flow ($\sim 0.119 \mu\text{l}/\text{min}$) was equal to the evaporation rate of water at room temperature with the air flow around 1 m/s measured in the lab ($\sim 0.113 \mu\text{l}/\text{min}$), and thus there was no visible evidence of leakage. At $\Delta P = 25$ psi, which provides a flow that is an order of magnitude higher ($\sim 1 \mu\text{l}/\text{min}$) than the evaporation rate, the leak source could be easily identified.

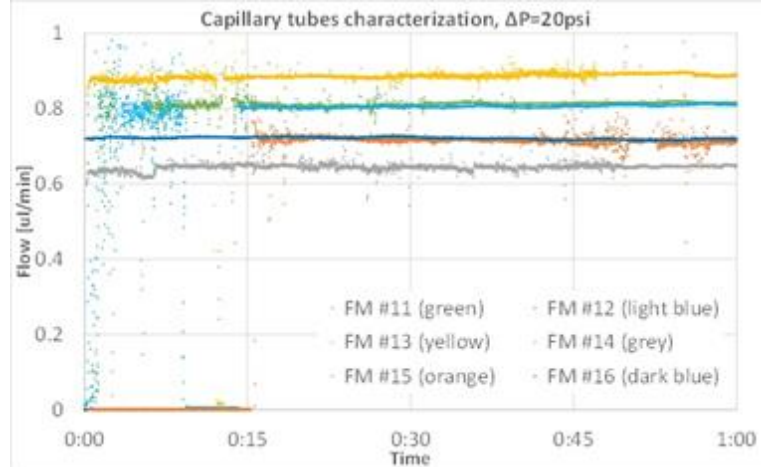


Figure 7. Capillary tubes and flow meters characterization test. Supply tank pressurized at 20 psig collecting tank open to the atmosphere. Time is in hh:mm.

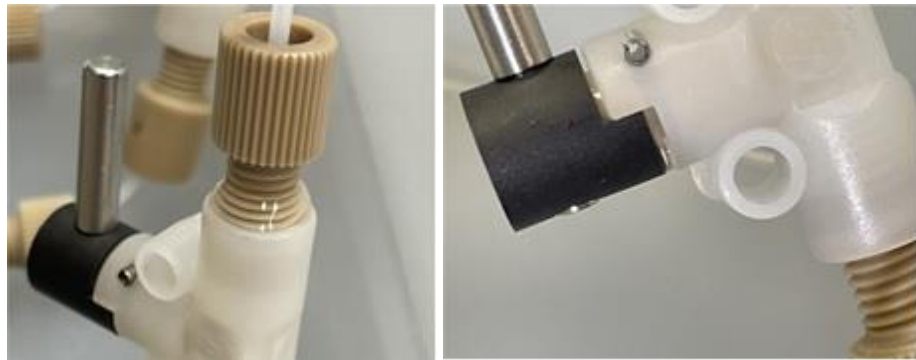


Figure 8. Leakage from stripped fitting (left) and body of shut-off valve (right).

III. Primary System Long-Term Testing

After completing the characterization of the system's main components, a long-duration testing campaign using the Primary DirectINJECT System was conducted to investigate mechanical reliability and mitigation techniques for potential failure modes. All six testbed were run with a delta P = 25 psi, which is the value necessary to achieve the desired theoretical flow of $1.0 \mu\text{l}/\text{min}$. Three supply tanks are connected to a pressure regulator set at 27.5 psig with their respective three primary collecting tanks connected to a pressure regulator set at 2.5 psig, and other three supply tanks are connected to a pressure regulator set at 55 psig with their respective three collecting tanks connected to a pressure regulator set at 30 psig. The DAQami and PowerShell programs were set to run the system continuously for 7 days at a time with no human action required after initiation, automatically saving the data in predetermined folders at the end of each 168-hour-period of testing. However, since the lab computer used for data acquisition kept randomly shutting down over-night, causing partial loss of data, the DAQami and PowerShell programs had to be stopped and restarted manually daily to avoid prolonged data losses and further delays.

During the third and fourth week of testing, three profiles showed a sudden decrease or increase in flow in two separate occasions. This happened in coincidence with the manual replenishment of the supply tanks with DI water and is due to the unintentional but unavoidable movement of the system which caused the capillary tubes to get bent or unbent from their previous equilibrium status. Thus, the Primary DirectINJECT System was re-designed to secure

all the components of the testbeds to a structural support frame and thus reduce their susceptibility to external mechanical forces. Moreover, the support clamping was modified to avert the deformation of the inner diameter of the tanks, which prevented some pistons from flowing down the barrels once they reached the level of the clamps. This modified design (see Figure 9) successfully prevented any accidental failures of the capillary tubes and electrical parts during tank-refill operations performed in the following 4 weeks of testing.



Figure 9. Upgraded Primary DirectINJECT System.

The summary of the 8-week-test of the Primary DirectINJECT System is shown in the graph in Figure 10. The red line represents the temperature profile, while each other line represents the flow profile of each one of the 6 channels. The gaps in the profiles throughout the entire 8 weeks, both for flow and temperature readings, are due to the data acquisition issues mentioned above. The variation of all the flow profiles over time closely follows the ambient temperature change, as expected. The average variation of flow over time in function of ambient temperature is $0.037 \mu\text{l}/\text{min}/^\circ\text{C}$, or 3.7% per 1°C .

The average variation of flow over time in function of ambient temperature is $0.037 \mu\text{l}/\text{min}/^\circ\text{C}$, or 3.7% per 1°C .

It was noticed, during the first week of testing, the flow of the 6 channels were all slightly offset from each other, however, all their profiles are almost identical. During the second week, two profiles (channels #5 and #6, light blue and green, respectively, in the graph in Figure 10) show a slowly decreasing flow, indicating possible partial plugging/degradation of the capillary tube. The sudden drop in flow seen at the beginning of the third day of the second week for the 3 testbeds supplied at 55 psig is due to the pressure drop caused by the temporary unplugging of the air compressor. Once plugged back in, the nominal flow values were restored. The sudden temperature spike towards the end of the second week followed by a temperature drop at the beginning of the third week was due to a failure of the building's HVAC. The sudden flow changes observed during the third and fourth week are due to the interference from external mechanical forces explained above, while the long-term, gradual decrease in flow for profile (testbed #4, yellow in the graph), might indicate a possible partial degradation of the capillary. The upgraded system reduced its susceptibility to external mechanical forces during the second half of the testing campaign, as desired. It also caused a sudden change in flow from the first 4-week run for some profiles, which was expected. The flows are shifted but their profiles over each 7-day run are almost identical. One profile (channel #3, grey in the graph), shows a continuous, slow decrease in flow during the last 4 weeks, indicating a potential long-term degradation of the capillary tube, with a total reduction in flow of about 28%. Another profile (channel #5, light blue in the graph) shows an initial more prominent decrease in flow from the beginning of week 5 to mid-week 7, followed by a sudden increase

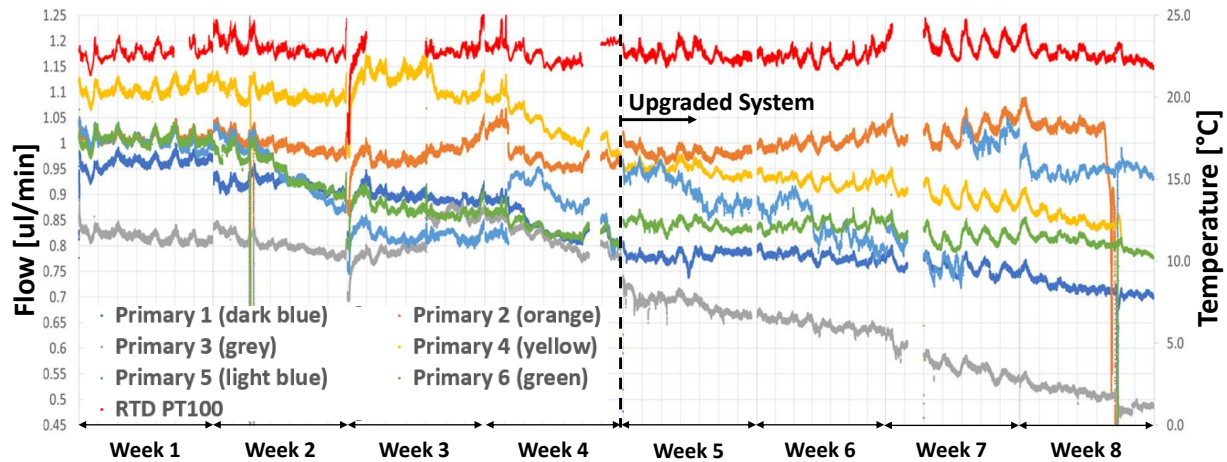


Figure 10. Summary of 8-week-test of the Primary DirectINJECT System, $\Delta P = 25$ psig.

in flow, which rebound back to its original value measured at the beginning of week 5 and was then remained stable until the end of the test. This behavior suggests that the capillary tube might have gotten partially plugged by some micrometer-size medium that eventually made its way out of it. One profile (testbed #2, orange in the graph), shows a continuous, slight increase in flow between week 5 and week 7, before stabilizing during week 8, for a total increase in flow of about 5%. Finally, two profiles (channels #2 and #4, orange and yellow, respectively, in the graph) show a sharp decrease in flow towards the end of the last week due to depletion of the feed solution in their respective supply tanks.

Overall, no failures were observed during the continuous 8-week testing campaign (4 weeks completed on the original testbed followed by 4 weeks on the upgraded system setup), demonstrating the simplicity of operations, with the only maintenance requirement being the replenishment of the supply tanks. Some profiles showed a long-term decrease while others showed an increase in flow not related to temperature variations, which will require further investigation and testing. The root causes of these trends could not be determined since the collected data isn't statistically sufficient to draw any conclusions on the hypothesized partial, short-term plugging of the capillary tube or its long-term degradation. Additional testing with the Primary DirectINJECT System will be continued during FY24. Moreover, a larger capillary testbed will be built to characterize a larger number of capillary tubes to obtain a statistical significant understanding of their behavior.

IV. System Leak Testing

After completing the characterization of the system's main components, a preliminary test using the Auxiliary System was conducted to investigate short-term, static leakage of the supply tanks pressurized with pistons. Six types of pistons with different designs and tolerances are available to ensure uniform dispensing force to provide accurate, consistent flow and to reduce waste, residue, and air entrapment. All six piston styles are made of high-density polyethylene. The white (general purpose "SmoothFlow", P/N 7366084) piston was used in this preliminary testing. It is characterized by a double-wiper design that creates a channel in between. The other available piston styles are the red (tight-fit, P/N 7366083) piston for use with mechanical dispensing equipment, the (beige loose-fit, P/N 7366076) piston optimized for air-entrapped fluids, the orange (flat-walled, P/N 7366082) piston with a looser fit to prevent bouncing when dispensing stringy, air-entrapped fluids, a blue (LV Barrier, P/N 7366078) piston used with very low viscosity fluids and finally, a clear (flexible, P/N 7366081) piston to reduce bouncing in viscous fluids (which will be excluded from future testing).

Both Auxiliary supply tanks were filled with 30 ml of dyed DI water so the tanks would be filled to about half height, corresponding to the maximum expected deformation of the shell, when pressurized. Both tanks were connected to the same pressure regulator, set at 30 psig, and the pressure was maintained constant for the entire duration of the experiment. The supply tanks were also maintained in a vertical position. The white "SmoothFlow" pistons were inserted in both tanks manually. During the insertion process, one of them required a much higher manual compression force, indicating likely different dimensional tolerances between the tanks and/or the pistons. Some water

got initially entrapped between the upper and lower wipers of the pistons (the groove) during the insertion process (Figure 11a). After pressuring the system, the entrapped water got evenly distributed in the groove along the contact perimeter between the lower wiper itself and the surface of the tank and is due to the non-airtightness across the upper wiper of the piston rather than to pure surface tension (Figure 11b). The system was inspected every 24 hours to identify new leaks or to measure the leak rates. After the first 24 hours, the water level within the groove decreased and after 48 hours it completely disappeared, indicating that it fully evaporated (Figure 12a). No leakages were observed over the following 48-hour period.



Figure 11a (left). Leakage in the piston channel after its insertion, tank not pressurized.

Figure 11b (right). Leakage in the channel after insertion and pressurization to 30 psig, time T = 0.

However, after 96 hours, leakage was observed in the groove of both tanks. The leaked volume was calculated at the end of the 7th day, resulting in about 4.4 μl (Figure 12b). Thus, the overall leak was $< 10 \mu\text{l}$ in each tank, meaning less than 1 ml/year.

Following this test, a Leak Testbed dedicated for long-term, large-scale testing of key system components (barrels, fittings, shut-off valves, and alternative pistons) was designed and already partially assembled. Figure 13 shows the first third of the Leak Testbed with the white SmoothFlow pistons and the red tight-fit pistons already installed. The supply tanks are laid horizontally to reduce the effect of gravity at the piston's wiper interface, thus, to better simulate microgravity conditions. The support clamping design was modified to prevent deformation of the inner diameter of the tanks, which would affect the tolerances between the tank's inner wall and the piston itself, thus causing leakage in both static and dynamic pressure conditions. The long-term testing of the Leak Testbed will be completed in FY24.

V. Bubbles Effect on Flow

A potential concern for capillary dosing systems is the formation of gas bubbles and their effect on the flow. The primary gas entry point in the DirectINJECT System would be at the piston/barrel interface in the supply tank, which may be subject to blow-by or cross diffusion of pressuring gas and water vapor due by differentials in partial pressures. A testing campaign was conducted on the Auxiliary System by supersaturating gas to induce bubble formation under extreme operational scenarios and investigate potential issues such as temporary or permanent flow reduction or interruption, and potential prevention and mitigation techniques. Bubbles form in solution following supersaturation of a dissolved gas due to either homogenous or heterogeneous nucleation. Homogenous nucleation, which is probably not feasible on the DirectINJECT System, typically occurs only if the difference between the ambient and dissolved gas pressure is greater than 1400 psi.⁴ In heterogeneous nucleation, bubbles form on microscopic surface imperfections, which lower the surface energy. The supersaturated dissolved gas diffuses into these bubbles, causing their growth and eventual detachment from the solid support. Heterogeneous bubble nucleation is the one expected to occur in the DirectINJECT System. The bubbles size and concentration depends on the number of nucleation sites, which generally increases in the presence of rough, hydrophobic surfaces. Other factors affecting bubble formation are the increase of gas supersaturation and of mixing intensity. Finally, bubble formation increases with temperature due to the decrease in gas solubility.

In this testing campaign, both supply tanks were filled with 30 ml of DI water saturated with air, with one set at 25 psig (low-pressure testbed) and the other set at 55 psig (high-pressure testbed). Their respective collecting tanks were set at 3 psig and 33 psig. The two testbeds, while maintaining the same ΔP of approximately 22 psi, are meant to simulate the two extreme operational scenarios that might be encountered on ISS. The ΔP was limited by the available pressure relief valves installed on the system. The capillary tubes were completely submerged in water in a

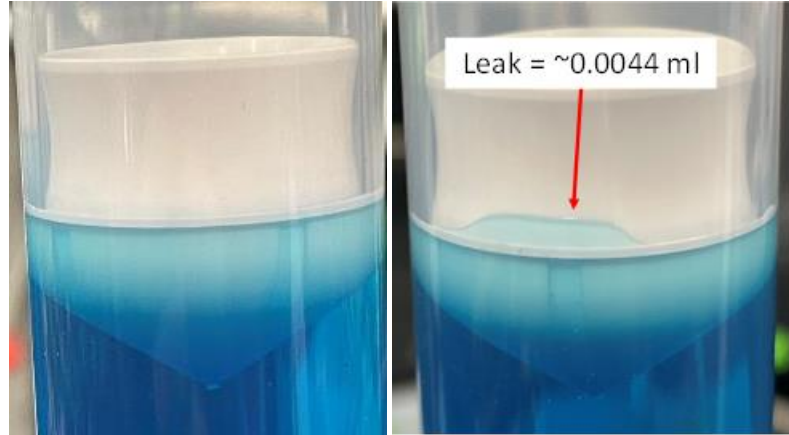


Figure 12a (left). Absence of any leakage in the channel of the piston at $T = 48$ hours, $P = 30$ psig.

Figure 12b (right). Leakage in the channel of the piston at $T = 168$ hours, $P = 30$ psig.

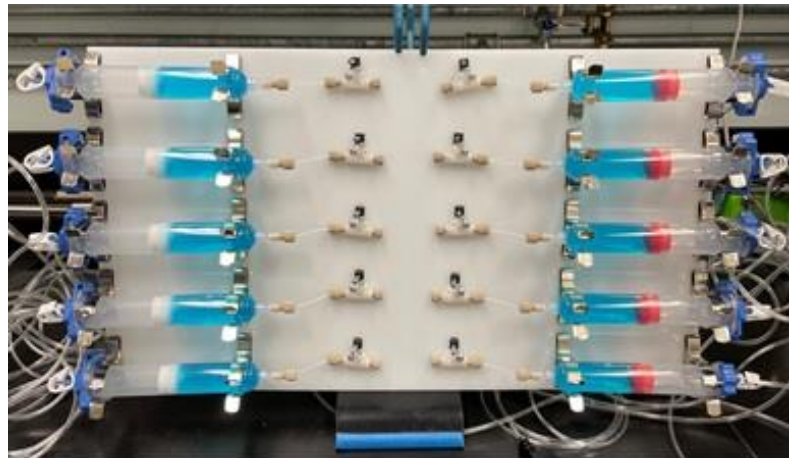


Figure 13. Preliminary assembly of the Leak Testbed.

heating bath, and the temperature of the water was set first at 20°C to obtain a baseline profile, and successively at 70°C, much higher than any operational temperature expected on a spacecraft. Due to the lower gas solubility at higher temperatures, bubble formation is expected to be higher at 70°C. A saturated N₂ solution was used for the preliminary experiments, however, due to the inability to order compressed gas cylinders during Covid, it was replaced with the much more available compressed air system. Even though air is more soluble in water than nitrogen, (0.024 g/kg for air vs. ~ 0.0138 g/kg for N₂ at 25°C and 14.7 psig) the difference shouldn't have a big impact on the outcome of the experiments. The capillary tubes were completely submerged in the heating bath horizontally first and vertically next (Figure 14a and 14b, respectively), to investigate possible effects of gravity on the flow of bubbles or bubble trains within the capillary. The experiments were run for 12 hours each, of which the first 4 hours were represented by the transient heating phase.

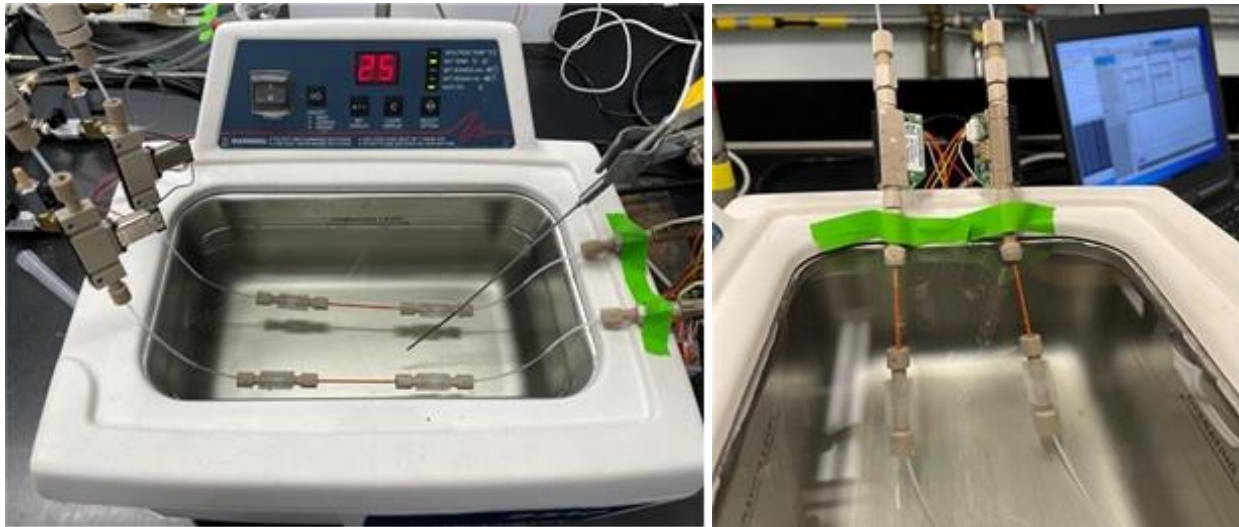


Figure 14a (left). Sonicator with Auxiliary capillary tubes submerged in horizontal configuration. Figure 14b (right). Auxiliary capillary tubes submerged in heating bath in vertical configuration.

No anomalies (bubble effects) were observed at 20°C in the horizontal experimental configuration. In the experiment in the vertical configuration (Figure 15), a few anomalies were observed. First, in the high P channel (Figure 15, light blue), there was a decrease in flow starting at 1hr. This decrease continued to increase (albeit very jaggedly) until at about 4.5hr it began to more rapidly decrease. This decrease continued until just after hour 5 when it suddenly increased. This behavior is not attributed to a gas bubble, but rather to some ultra small particulate which entered, bounced around, and then finally exited the capillary tube. If we now focus on the low P channel (Figure 15, dark blue), a slow and steady decrease in flow is observed. This could possibly be a bubble effect. If a bubble nucleated and then grew within the capillary, there would be a slow constriction of the flow channel giving a very slow decrease in flow rate as is observed. This bubble, could be slowly pushed through the capillary as it grew until it reaches the end of the capillary at which point the flow through the capillary would be rapidly restored, as is observed at about 3.5 hrs into the experiment. After hour 3.5, a slow decrease is again observed which could be the beginning of another gas bubble. This result implies that if gas bubble formation does occur, that its effect is less than 1% of the total flow rate and so would have no effect on the reliability of the process.

Finally, if there was a large air bubble which entered the capillary, since its dynamic viscosity at room temperature and atmospheric

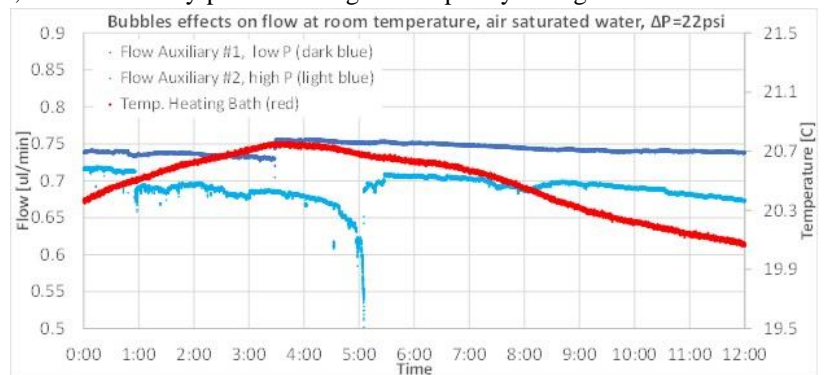


Figure 15. Bubbles effect on flow rate of DI water supersaturated with air at room temperature with capillary tubes in a vertical configuration, $\Delta P = 22$ psi. Time is in hh:mm.

pressure (1.8×10^{-5} Pa-s) is about $1/50^{\text{th}}$ that of water (10^{-3} Pa-s), it would flow through the capillary tube about 50 times faster than water, based on Eq. (1). Thus, any large bubbles which enter the capillary would quickly pass and not introduce any issues, i.e. if an improbably 1 mL gas bubble did somehow form and pass through the capillary, the effect would be to produce only 2L of “untreated” water which when mixed with “treated” water would result in an average Ag biocide concentration over a 1 hr period of 264 ppb (still within the 400-200 ppb range), but the average over an 8 hr process would still give an average Ag biocide concentration of 383 ppb.

At $\sim 70^{\circ}\text{C}$, scatter was observed in the recorded flow data both for the horizontal and the vertical configurations (Figure 16). If this scatter is due to the presence of micro/nano bubbles, this indicates that they do not affect the overall performances of the system since the average flow was in line with the expected theoretical value. A more probable explanation of this scattered data is that the type of flow meter used in the DirectINJECT System is a calorimetric flow meter calibrated for H_2O at 23°C . By nature, its accuracy is

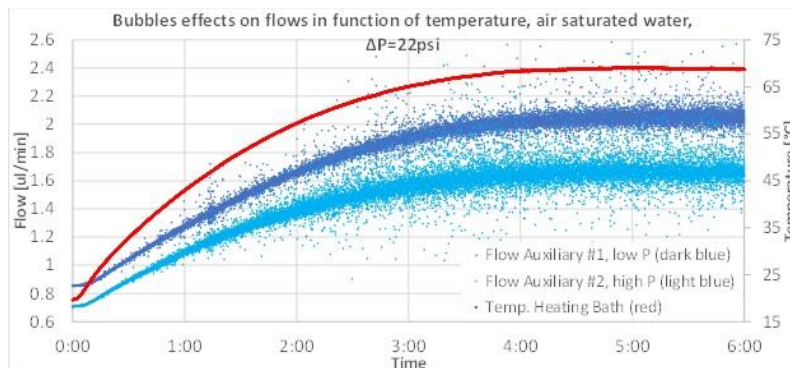


Figure 16. Flow rates of DI water in function of its temperature with capillary tubes in a vertical configuration, $\Delta P = 22$ psi. Time is in hh:mm.

affected by variations in temperature, heat capacity, and viscosity of the fluid. The flow meter is subject to an error of 0.09% of the measured value / $^{\circ}\text{C}$ (according to the manufacturer). The flow meter measures the asymmetrical temperature of a fluid flow between two temperature sensors, respectively mounted upstream and downstream of a heating element in the direction of flow. The higher the temperature of the flowing media, the smaller is the difference in temperature between the two sensors, and thus the higher the error. Moreover, at $\sim 70^{\circ}\text{C}$, the temperature of the water flowing across the meter exceeded the operational temperature range recommended by the manufacturer, which is between 10°C and 50°C , with maximum short-term temperature peaks of 60°C .

In conclusion, bubble formation does not affect the functionality nor performance of the DirectINJECT System. Moreover, the potential permeation of gas at the piston/barrel interface in the supply tank could be further mitigated by an improved piston seal, which should be achieved with the red tight-fit piston that will be tested in FY24. Any other available bubble separation and trapping techniques are unnecessary and they would introduce additional complexity.

VI. Future Work

Long-term, static experiments will be conducted on the Leak Testbed to down-select the best piston among the 5 available alternative options, and to identify and quantify any leakages in the supply tanks and in the shut-off valves. Long-term testing will be conducted on the Primary DirectINJECT System using the down-selected piston to investigate mechanical reliability of all the system components and to verify materials compatibility using AgNO_3 solution. The Auxiliary DirectINJECT System will be used to perform short-term experiments to investigate any phenomena that we will observe during the long-duration testing campaigns, and to test mitigation techniques or alternative system components or design modifications.

In parallel, a new Capillary Characterization System will be assembled to quantify performance degradation of the capillary tubes over time, if any, and to collect enough data to allow to demonstrate our hypotheses with statistical significance. A new Solenoid Valve Testbed will also be built to test long-term reliability of the solenoid valves subject to accelerated power cycling. Finally, the assembly of the ISS-Like DirectINJECT Prototype System will be operated daily over several months under the same range of conditions expected for the Water Processor Assembly system on ISS (flow rates and pressures) to conduct long-term testing of the AgNO_3 concentration in the dosed solution and to prove the robustness of the system design.

Acknowledgments

We acknowledge the Mars Campaign Office for financial support.

References

¹Vance, J., Delzeit, L., “DirectINJECT: Dosing Systems for Concentrated Liquid Biocides,” *51st International Conference on Environmental Systems*, ICES-2022-9, 10-14 July 2022, Saint Paul, Minnesota.

²https://www.esa.int/ESA_Multimedia/Images/2021/08/Temperatures_on_the_Space_Station

³<https://sensirion.com/products/technology/>

⁴Harvey, H. H., “Gas Disease in Fishes—A Review.” *Proceedings of Chemistry and Physics of Aqueous Gas Solutions.*, Electrothermics and Metallurgy and Industrial Electrolytic Divisions, Electrochemical Society, Princeton, N.J., 1975, pp. 450-485